

DOI: 10.1002/open.201200045

Carbon Dioxide Adsorption in Betulin-Based Micro- and Macroporous Polyurethanes

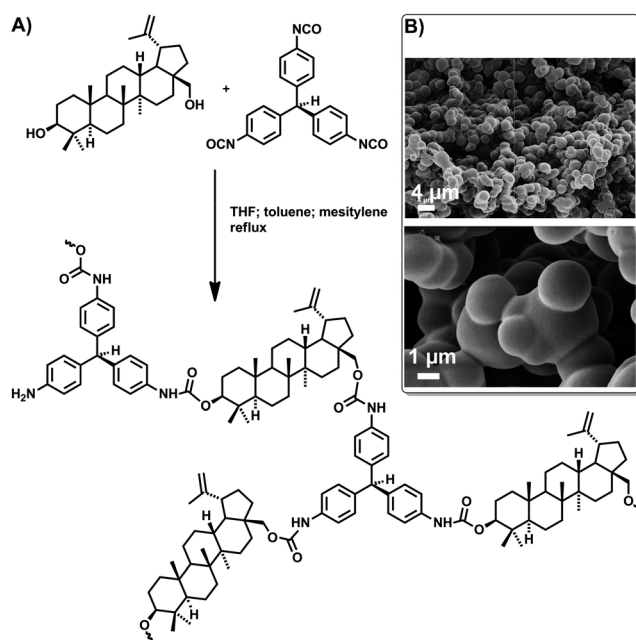
Jekaterina Jeromenok,^[a] Winfried Böhlmann,^[b] Christian Jäger,^[c] and Jens Weber^{*[a]}

Microporous polymers, that is polymers having pores of molecular size ($D < 2$ nm), attracted a lot of interest during the last few years.^[1–4] They are promising materials for gas storage or separation but could also find use in heterogeneous catalysis. Recently, the separation of the green house gas CO₂ evoked large interest in the scientific community. Among other microporous materials, such as activated carbon,^[5–7] metal-organic frameworks,^[8–10] or zeolites,^[11] nanoporous polymers have been suggested as adsorbents,^[12–17] as they can combine large surface areas together with the well-known processability of common polymers. Within this contribution, we present microporous polyurethane with good CO₂ over N₂ selectivity. The state of CO₂ adsorbed in the micropores is analyzed by NMR spectroscopy in order to get a better picture of the gas–polymer interactions, which have not been subject to intense investigations so far. In combination with the analysis of the adsorption data, this allows a statement on the underlying basics of the high selectivity.

One of the various ways to synthesize microporous polymers starts from the concept of intrinsic microporosity. Using stiff and contorted molecules, it is possible to prevent dense packing of the polymer chains, leaving an extraordinary high free volume behind. If the free volume is connected and can be accessed from the environment, the polymer is considered to be intrinsically microporous.^[18,19] Recently, we developed microporous polyesters with promising CO₂/N₂ selectivity based on betulin.^[20] Betulin, a triterpene that can be extracted from birch bark in up to 30% yield with respect to the dry weight of the bark, can be used as a building block for microporous polymers. Two hydroxy groups point out of the otherwise stiff hydrocarbon plane, thus introducing frustrated packing (=high free volume) upon polymerization. Consequently, we envisaged the synthesis of microporous polyurethanes as a next

step, making use of the diol nature of betulin. Polyurethanes based on betulin have already been described in the 1980s by Russian and Finnish researchers, but no investigations were performed on the porosity of the products.^[21]

Here, we targeted the synthesis of microporous networks, as these can typically result in higher porosities. Hence, a commercial triisocyanate (20% triphenylmethane triisocyanate in ethyl acetate, Desmodur® RE, Bayer AG) was used as a crosslinker in an A₃-B₂ polyaddition reaction to prepare microporous polymer networks (see Scheme 1). Betulin was extracted from birch bark and recrystallized from ethanol before use.



Scheme 1. A) Chemical structures of betulin and triphenylmethane triisocyanate and the corresponding polyurethane network. B) SEM micrographs of the morphology of the resulting networks.

The reaction was performed at boiling temperature in various solvents such as tetrahydrofuran (THF), toluene or mesitylene. The polymer precipitated out of solution as the reaction proceeded, typically as interconnected microglobules of less than 10 μm diameter (see Scheme 1B). Such morphology is typically observed and used in monolithic polymer materials used for separation applications, as it allows fast mass transfer.

Dry solvents can be used in order to prevent potential foaming due to the formation of CO₂ and significant amounts of urea linkages. Foaming could interfere with the intrinsic porosity introduced by the betulin stereochemistry as discussed earlier. However, no strong difference was observed between the

[a] Dr. J. Jeromenok, Dr. J. Weber
Department of Colloid Chemistry
Max Planck Institute of Colloids and Interfaces, Science Park Golm
14424 Potsdam (Germany)
E-mail: jens.weber@mpikg.mpg.de

[b] Dr. W. Böhlmann
University of Leipzig, Faculty of Physics and Geosciences
Linnéstr. 5, 04103 Leipzig (Germany)

[c] Prof. Dr. C. Jäger
BAM Federal Institute for Materials Research and Testing, Division 1.3
Richard Willstaetter Str. 11, 12489 Berlin (Germany)

Supporting information for this article is available on the WWW under <http://dx.doi.org/10.1002/open.201200045>.

© 2013 The Authors. Published by Wiley-VCH Verlag GmbH & Co. KGaA. This is an open access article under the terms of the Creative Commons Attribution Non-Commercial License, which permits use, distribution and reproduction in any medium, provided the original work is properly cited and is not used for commercial purposes.

outcomes of reactions performed in dry or analytical grade solvents. Nevertheless, dry toluene was used to prepare the sample named Bet-PUR-1, which will be discussed in detail in the following.

The chemical identity of the networks was confirmed by FTIR and solid-state NMR spectroscopy. FTIR indicated the successful formation of the urethane linkage as evidenced by the reduction of hydroxy vibrational modes at $\tilde{\nu} > 3000 \text{ cm}^{-1}$ and the rise of a broad carbonyl band at 1702 cm^{-1} and an amide NH-bending mode at 1592 cm^{-1} . Solid-state ^1H - ^{13}C cross-polarization magnetic angle spinning (CPMAS) spectroscopy can also confirm the urethane formation (Figure 1B). The carbonyl

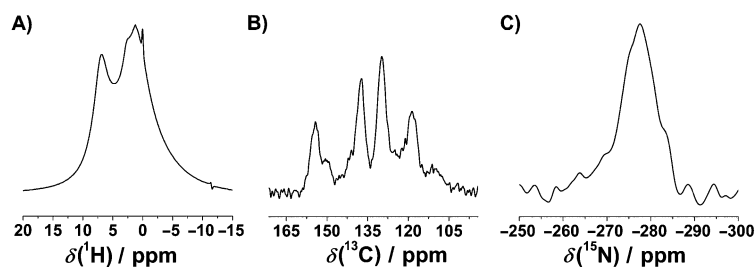


Figure 1. A) Solid-state ^1H NMR spectrum, B) solid-state ^1H - ^{13}C CPMAS NMR spectrum and C) solid-state ^1H - ^{15}N CPMAS NMR spectrum of a botulin-based polyurethane network (Bet-PUR-1).

C atom causes a peak at a chemical shift of $\delta = 154 \text{ ppm}$. The accompanying shoulder of this peak can be attributed to the tertiary C atom of the isobutylene unit of betulin. The peaks at δ values of ~ 137 , ~ 130 and $\sim 119 \text{ ppm}$ can be attributed to the aromatic C atoms of the Desmodur[®] RE unit, while the peak at $\delta = 110 \text{ ppm}$ is also due to the isobutylene unit. The peaks at δ values of $\sim 82 \text{ ppm}$ and $\sim 63 \text{ ppm}$ can be attributed to the oxygen bearing C atoms of betulin. The peaks at lower chemical shift are due to the aliphatic betulin backbone and the tertiary C atom of the Desmodur[®] RE unit, which however cannot be distinguished within the spectrum.

Thermal analysis of the networks under an N_2 atmosphere showed a two-step decomposition. At $\sim 110^\circ\text{C}$, solvent loss is observed. Decomposition begins at 350°C with a very sharp mass loss of 42% followed by a second broad decomposition step at 590°C . Differential scanning calorimetry (DSC) of the freeze-dried network did not show any phase transition or glass point within a temperature range from room temperature up to 125°C , indicating a stable operation range for adsorption applications.

The porosity of the formed polymer networks was investigated by gas adsorption/desorption measurements using N_2 and CO_2 as adsorbates.^[22,23] N_2 adsorption at 77.3 K could not reveal any pronounced microporosity of the polymer networks ($S_{\text{BET}} \sim 5 \text{ m}^2\text{g}^{-1}$), irrespective of the applied drying method (freeze-drying or evaporative drying). The absence of measurable microporosity at 77.3 K could be due to partial pore closure as a consequence of hydrogen bonding but also due to restricted access of N_2 at 77.3 K into the narrow pores because of diffusional problems.^[24] It was shown in previous studies that intermolecular interactions can indeed lead to reduction

of pore sizes by elastic deformations.^[23] In the present case, the asymmetric shape of the peak originating from the urethane nitrogen as observed in the ^1H - ^{15}N CPMAS NMR spectrum indicates that there are indeed additional interactions. The peak shows at least two shoulders, which could indicate the presence of hydrogen-bonded structures. This would also be supported by the rather broad C=O and N-H peaks within the IR spectra, which could be due to overlapping of "free" and hydrogen-bonded moieties.^[25] However, at the current state, we cannot exclude the presence of urea or biuret functionalities. As dry solvents have been used, we are however confident that they would be small in number and not solely be responsible for the broadened and anisotropic peaks observed by spectroscopy.

Additional porosity analysis was undertaken by CO_2 adsorption at 273 and 283 K as well as N_2 adsorption at 273 K . This set of experiments allows to detect microporosity and to calculate apparent gas selectivities and CO_2 adsorption strength. It was shown previously that CO_2 can enter very small pores in polymers or carbons that otherwise could not be detected.^[20,24,26]

The CO_2 uptake of Bet-PUR-1 at 273 K and 1 bar was around 1.26 mmol g^{-1} ($5.5 \text{ wt}\%$; see Figure 2A) indicating moderate microporosity. Using models developed for carbons,^[27] it is possible to determine the specific surface area ($S \sim 300 \text{ m}^2\text{g}^{-1}$) and the pore size distribution (PSD, see the Supporting Information). The majority of pores seem to have pore sizes between 0.5 and 1 nm . Such

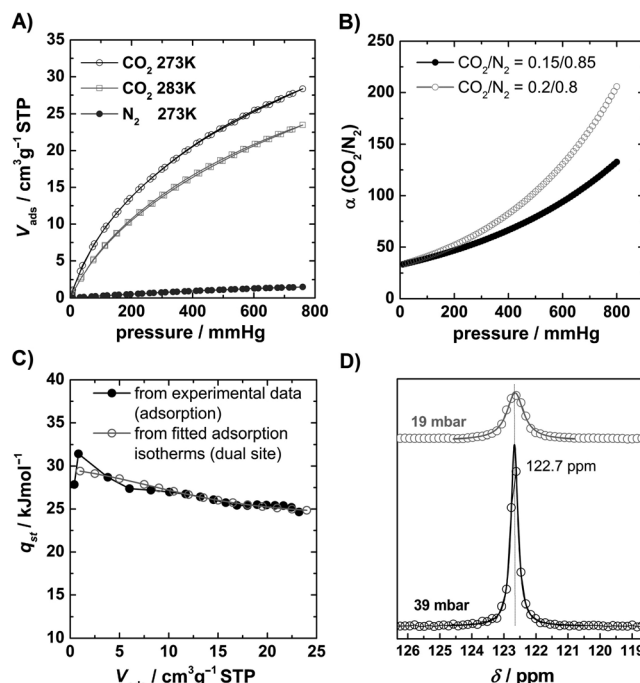


Figure 2. A) CO_2 (273 and 283 K) and N_2 (273 K) adsorption isotherms on Bet-PUR-1. B) IAST prediction of the CO_2/N_2 selectivity (273 K) for a $0.2:0.8$ and a $0.15:0.85$ gas composition. C) Isothermic heat of adsorption q_{st} calculated directly by the AS1Win software and calculated based on the fitted isotherms. D) ^{13}C NMR spectra of ^{13}C - CO_2 confined within Bet-PUR-1.

small pore sizes can be interesting for kinetic gas separations. CO₂ is known to have a smaller kinetic diameter than N₂ and a separation based on kinetic restrictions can be imagined. The N₂ uptake at 273 K and 1 bar was 0.065 mmol g⁻¹. The adsorption isotherms could be fitted using a dual or single-site Langmuir model in the case of CO₂, while a simple Langmuir fit was sufficient to fit the N₂ isotherm (see the Supporting Information for full fit details). Based on the fit data, it is possible to calculate the CO₂/N₂ selectivity using the ideal adsorbed solution theory (IAST) approach. A selectivity of ~130 can be calculated for a gas composition of 15% CO₂ and 85% N₂ at 273 K and 800 mmHg. This is a high value, which must however be placed into relation to the capacity, which is lower than that of other microporous polymers, following the trade-off relation between capacity and selectivity.^[28] Nevertheless, the preliminary results are encouraging for further study of the gas separation properties of betulin-based polyurethanes.

An advantage amongst other approaches towards microporous polymers lies in the fact that the engineering of polyurethanes into usable morphologies (e.g., monolithic foams) is well-developed, which could support the manufacturing of prototypes for real separation applications.

Another question, which needs to be tackled, is related to the nature of adsorbed CO₂. There is an ever increasing number of microporous polymeric materials, which shows no N₂ uptake at 77.3 K but CO₂ uptake at 273 K. This brings up the question, whether CO₂ is indeed physisorbed into micropores or if it undergoes chemical interactions leading to the observed uptake. In the present case, free amines could interact with CO₂, and a strong interaction could also be imagined between CO₂ and the amide N–H. A first way to screen potential interactions is the calculation of the isosteric heat of CO₂ adsorption (q_{st} , Figure 2C). These can be derived directly from the commercialized software, but also from the fitted isotherms (Clausius-Clapeyron approach). Both data sets agree well, and values of ~30 kJ mol⁻¹ are calculated for zero loading. These decrease to ~25 kJ mol⁻¹ at higher loadings, indicative of pure physisorption of CO₂ within the micropores of the betulin-based polyurethane. The slightly higher heat of adsorption at low coverage can be due to pore size effects; that is, very small pores give rise to increased wall-adsorbate interactions and/or to the presence of polar sites (urethane linkages) that also have stronger interactions with CO₂. To further characterize the state of CO₂ adsorbed into small pores, solid-state ¹³C NMR spectra of ¹³C-CO₂ confined to the pores were recorded (Figure 2D). ¹³C-CO₂ was loaded into an NMR tube containing Bet-PUR-1, and the tube was sealed. Low pressures (< 50 mbar) were used to gain information about the low coverage region. The spectra show isotropic peaks at a position of 122.7 ppm, which is comparable to values found for microporous activated carbon (118–123 ppm).^[29] The value is indicative of CO₂, which is confined but still can undergo isotropic rotations, that is purely physisorbed CO₂. Studies on CO₂ confined in extremely narrow micropores (activated carbon fibres, width < 0.42 nm) showed that a second peak originates at lower chemical shift, which is extremely broad as a consequence of restricted uniaxial rotation. Such a peak was not visi-

ble in our case, which can be interpreted as the absence of extremely small pores. Hence, the higher heat of adsorption at low coverage can be attributed to the polar urethane moieties, which are preferential adsorption sites to CO₂ compared to the unipolar aliphatic betulin backbone.

In summary, an in-depth study on the characterization of betulin-based polyurethanes was presented. Betulin, which is a renewable resource and not in conflict with food production, can be used as a structure-directing monomer in an A₂+B₃ synthesis. Reaction with a commercial isocyanate results in a microporous polymer containing ~64 wt% renewable material. The synthesis can be conducted in a variety of solvents, typically resulting in a structure of interconnected microglobules. Such a structure is commonly found in macroporous polymeric monoliths.^[30] Indeed, using THF as solvent, a monolithic structure could be obtained when the reaction was performed without stirring. The monolith ruptured upon conventional drying (see the Supporting Information), which is a common problem of monolithic materials and could most probably be prevented by supercritical drying. Nevertheless, this is encouraging for further engineering work on this type of polymers. The adsorption studies revealed a promising CO₂/N₂ gas selectivity based on the analysis of single gas adsorption isotherms. The overall capacity is not very high compared to other systems, but this could be compensated by the better processability. No binders are potentially required to form monoliths, which is advantageous compared to powder processing. The selectivity could be a result of rather small pores (kinetic separation effect),^[11] as no specific interactions could be evidenced by in situ NMR spectroscopy. The presence of the urethane linkages resulted presumably in the formation of hydrogen bonds, which are known to reduce pore sizes.

Experimental Section

General: Betulin was obtained from extraction of birch bark (*Betula pendula*) with CH₂Cl₂, followed by recrystallization from EtOH as described earlier.^[20]

Elemental analyses were done with a varioMicro elemental analysis instrument (Elementar Analysensysteme, Hanau, Germany). Thermogravimetric analyses were performed in synthetic air atmosphere with a NETZSCH TG209 F1 instrument (Selb, Germany) at a heating rate of 10 K min⁻¹. Differential scanning calorimetry (DSC) was performed using a Mettler-Toledo instrument under N₂ atmosphere and a heating rate of 10 K min⁻¹. Fourier transform infrared spectra (FTIR) were collected using a BIORAD FTS 6000 FTIR spectrometer under attenuated total reflection (ATR) conditions. Scanning electron microscopy (SEM) measurements were carried out using a LEO 1550-Gemini electron microscope (acceleration voltage: 3 kV). For SEM measurements the samples were coated with a thin gold layer (approx. 2 nm).

Gas sorption: Nitrogen sorption experiments were conducted at 77.3 K using Quadrasorb and Autosorb 1-MP from Quantachrome Instruments (Boynton Beach, FL, USA). Data evaluation was done by means of different methods in the Quantachrome programs AS1win and QuadraWin. CO₂ and N₂ at 273 K and 283 K were done using Autosorb 1-MP from Quantachrome Instruments. Isothermic heats of adsorption were calculated using the AS1Win software

provided by Quantachrome Instruments as well as from fits of the isotherms. Before all adsorption experiments, the samples were degassed overnight at 353 K under dynamic vacuum. High purity gases were used for all measurements.

NMR spectroscopy: Solid state ^{13}C magic angle spinning (MAS) NMR measurements under $^{13}\text{CO}_2$ atmosphere were performed on a Bruker Avance 400 spectrometer at a resonance frequency of 100.61 MHz and a spinning frequency of 10 kHz. Adamantane was used as external standard (signals at 28.1 and 37.5 ppm). Solid-state NMR experiments were performed on a BRUKER Avance 400 spectrometer (9.4 T). Experiments were carried out at RT using a 2.5 mm MAS sample BRUKER double resonance probe for solid-state ^1H and ^{13}C NMR. ^1H MAS NMR spectra (400.2 MHz) were run with rotor-synchronized echo detection for suppressing probe background signals using a MAS frequency of 25 kHz. ^1H 90° pulse lengths of $3.3\ \mu\text{s}$ were used with repetition times of 3 s, and 16 scans were accumulated. ^1H chemical shifts were referenced versus trimethylsilane (TMS) using adamantane as external secondary standard ($\delta = 1.78$ ppm). ^1H - ^{13}C cross polarization (CP)MAS experiments were carried out using the same 2.5 mm MAS probe, but the sample spinning frequency was 12.5 kHz. Spectra were recorded using a ^1H 90° pulse length of $3.3\ \mu\text{s}$, a contact time of 2 ms and a repetition time of 3 s. The ^{13}C spin lock field was held constant while the ^1H spin lock field was ramped down to 50% of its initial value. 16k scans were accumulated, and high-power proton decoupling was carried out with a 15° two pulse phase modulation (TPPM) sequence.^[31] Similarly, ^1H - ^{15}N CPMAS spectra were acquired using a BRUKER 7 mm MAS probe for sensitivity reasons. The sample spinning frequency was 5 kHz. Spectra were recorded with a ^1H 90° pulse length of $5\ \mu\text{s}$, a contact time of 1 ms and a repetition time of 3 s. Again, the ^{15}N spin lock field was held constant while the ^1H spin lock field was ramped down to 50% of its initial value. 20000 scans were accumulated with proton TPPM decoupling as described earlier. ^{15}N chemical shifts (δ) are reported relative to CH_3NO_2 with NH_4Cl as secondary standard ($\delta = -341$ ppm).

Typical synthesis of a polyurethane network (Bet-PUR-1): A 20% solution of triphenylmethane triisocyanate in EtOAc (1.1 mL, 297 mg, 0.8 mmol; Desmodur[®] RE solution, Bayer AG) was introduced to a solution of betulin (531 mg, 1.2 mmol) in toluene (12 mL) at 110°C . The mixture was held at reflux for 1.5 h. A brownish precipitate was formed after 15 min, gradually changing its color to violet. The precipitate was extracted with tetrahydrofuran (THF; Soxhlet) for 20 h and dried in vacuo at 60°C to give Bet-PUR-1 as a white-pink powder (675 mg, 92%): FTIR (ATR): $\tilde{\nu} = 3300$ (broad, O–H), 2920 (weak, $\text{C}_{\text{sp}^3}\text{–H}$), 2835 (weak, $\text{C}_{\text{sp}^3}\text{–H}$), 1709 (strong; C=O), 1592 (medium, N–H), 1485 (strong, C=C), 1385 (weak), 1280 (medium), 1180 (medium), 1020 (medium), $990\ \text{cm}^{-1}$ (weak).

Synthesis of a polyurethane monolith: After dissolving betulin (267 mg, 0.6 mmol) in THF (3 mL) at RT in a Schlenk flask, Desmodur[®] RE solution (0.6 mL, approx. 0.44 mmol) was added, and the mixture was stirred shortly. The stirring bar was removed, and the reaction mixture was aged at 70°C for 7 d. The resulting purple monolith was washed with THF and dried in vacuo at 60°C , yielding 409 mg (95 wt %).

Acknowledgements

We thank Bayer AG for a donation of Desmodur[®] RE. Jessica Brandt is acknowledged for lab assistance. The Max-Planck Society is acknowledged for financial support.

Keywords: carbon dioxide · gas adsorption · microporous polymers · renewable resources · solid state NMR spectroscopy

- [1] A. Thomas, P. Kuhn, J. Weber, M. M. Titirici, M. Antonietti, *Macromol. Rapid Commun.* **2009**, *30*, 221–236.
- [2] A. Thomas, *Angew. Chem.* **2010**, *122*, 8506–8523; *Angew. Chem. Int. Ed.* **2010**, *49*, 8328–8344.
- [3] N. B. McKeown, P. M. Budd, *Macromolecules* **2010**, *43*, 5163–5176.
- [4] R. Dawson, A. I. Cooper, D. J. Adams, *Prog. Polym. Sci.* **2012**, *37*, 530–563.
- [5] L. Yu, C. Falco, J. Weber, R. J. White, J. Y. Howe, M.-M. Titirici, *Langmuir* **2012**, *28*, 12373–12383.
- [6] M. Sevilla, A. B. Fuertes, *Energy Environ. Sci.* **2011**, *4*, 1765.
- [7] C. Pevida, T. C. Drage, C. E. Snape, *Carbon* **2008**, *46*, 1464–1474.
- [8] K. Sumida, D. L. Rogow, J. A. Mason, T. M. McDonald, E. D. Bloch, Z. R. Herm, T.-H. Bae, J. R. Long, *Chem. Rev.* **2012**, *112*, 724–781.
- [9] Y. Bae, R. Q. Snurr, *Angew. Chem.* **2011**, *123*, 11790–11801.
- [10] F. Debatin, K. Behrens, J. Weber, I. A. Baburin, A. Thomas, J. Schmidt, I. Senkovska, S. Kaskel, A. Kelling, N. Hedin, *Chem. Eur. J.* **2012**, *18*, 11630–11640.
- [11] Q. Liu, A. Mace, Z. Bacsik, J. Sun, A. Laaksonen, N. Hedin, *Chem. Commun.* **2010**, *46*, 4502–4504.
- [12] R. Dawson, L. A. Stevens, T. C. Drage, C. E. Snape, M. W. Smith, D. J. Adams, A. I. Cooper, *J. Am. Chem. Soc.* **2012**, *134*, 10741–10744.
- [13] N. Du, H. B. Park, G. P. Robertson, M. M. Dal-Cin, T. Visser, L. Scoles, M. D. Guiver, *Nat. Mater.* **2011**, *10*, 372–375.
- [14] A. Wilke, J. Weber, *J. Mater. Chem.* **2011**, *21*, 5226.
- [15] M. G. Rabbani, H. M. El-Kaderi, *Chem. Mater.* **2012**, *24*, 1511–1517.
- [16] Q. Chen, M. Luo, P. Hammershøj, D. Zhou, Y. Han, B. W. Laursen, C.-G. Yan, B.-H. Han, *J. Am. Chem. Soc.* **2012**, *134*, 6084–6087.
- [17] A. Wilke, J. Yuan, M. Antonietti, J. Weber, *ACS Macro Lett.* **2012**, *1*, 1028–1031.
- [18] P. M. Budd, B. S. Ghanem, S. Makhseed, N. B. McKeown, K. J. Msayib, C. E. Tattershall, *Chem. Commun.* **2004**, 230–231.
- [19] J. Weber, O. Su, M. Antonietti, A. Thomas, *Macromol. Rapid Commun.* **2007**, *28*, 1871–1876.
- [20] J. Jeromenok, W. Böhlmann, M. Antonietti, J. Weber, *Macromol. Rapid Commun.* **2011**, *32*, 1846–1851.
- [21] V. A. Erä, P. Jääskeläinen, K. Ukkonen, *Angew. Makromol. Chem.* **1980**, *88*, 79–88.
- [22] J. Weber, J. Schmidt, A. Thomas, W. Böhlmann, *Langmuir* **2010**, *26*, 15650–15656.
- [23] J. Weber, N. Du, M. D. Guiver, *Macromolecules* **2011**, *44*, 1763–1767.
- [24] N. Ritter, I. Senkovska, S. Kaskel, J. Weber, *Macromolecules* **2011**, *44*, 2025–2033.
- [25] M. M. Coleman, K. H. Lee, D. J. Skrovaneck, P. C. Painter, *Macromolecules* **1986**, *19*, 2149–2157.
- [26] D. Lozano-Castelló, D. Cazorla-Amorós, A. Linares-Solano, *Carbon* **2004**, *42*, 1233–1242.
- [27] A. Vishnyakov, P. I. Ravikovitch, A. V. Neimark, *Langmuir* **1999**, *15*, 8736–8742.
- [28] R. Dawson, T. Ratvijitvech, M. Corker, A. Laybourn, Y. Z. Khimyak, A. I. Cooper, D. J. Adams, *Polym. Chem.* **2012**, *3*, 2034–2038.
- [29] H. Omi, T. Ueda, K. Miyakubo, T. Eguchi, *Appl. Surf. Sci.* **2005**, *252*, 660–667.
- [30] M. R. Buchmeiser, *Polymer* **2007**, *48*, 2187–2198.
- [31] A. E. Bennett, C. M. Rienstra, M. Auger, K. V. Lakshmi, R. G. Griffin, *J. Chem. Phys.* **1995**, *103*, 6951–6958.

Received: November 26, 2012

Published online on January 18, 2013